

Cu^{II}-Materials — Crystal Chemistry Meets Magnetism

Helge Rosner, Michelle Dawn Johannes¹, Stefan-Ludwig Drechsler², Walter Schnelle, Wei Liu, Ya-Xi Huang, and Rüdiger Kniep

The general structural element of Cu(II)-oxygen compounds is the square planar CuO₄ unit which is shown in Fig. 1 together with the relevant covalent orbitals. The valence electron configuration of Cu²⁺ is 3d⁹4s⁰, and that of the O²⁻ ion is 2p⁶. The highest occupied atomic orbitals are Cu 3d orbitals and O 2p orbitals. Most of these orbitals are non-bonding. There is one sigma orbital at each ion with the angular dependencies of the wave function given by $(x^2-y^2)/r^2$ for the Cu 3d orbital and by x/r and y/r for the O 2p orbital, respectively. The relevant molecular orbital energy level scheme (Fig. 1) shows that the strong covalent $d-p$ bond leads to an energy splitting between the bonding and antibonding levels as large as 10 eV. The fully occupied nonbonding Cu 3d and O 2p levels are in between. Because one electron is missing com-

pared to fully occupied 3d and 2p shells, the antibonding dp -level must be half filled. Due to a strong intra-atomic correlation present in the Cu 3d-orbitals, the molecular field approximation is, however, not sufficient to describe the electronic properties, and the half-filled antibonding level splits due to these correlations into a lower and an upper so called Hubbard level. Thus, these strong correlations are responsible for the insulating behavior of undoped cuprates. According to the occupation of the molecular levels shown in Fig. 1, the CuO₄ unit is magnetically active, carrying a spin 1/2. Due to this small and localized moment compounds with CuO₄ units are ideal objects to study the effect of quantum fluctuations.

General interest in magnetically low-dimensional systems began with the advent of quantum mechanics and the development of spin-spin interaction models in order to explain the magnetic behavior. Though deceptively simple, early models such as Ising- and Heisenberg-models have exact ground state solutions [1] only in one or two dimensions (1D or 2D). The search for real materials with substantially 1D or 2D magnetic interactions initially had the purpose of verifying or disproving theoretical predictions of exotic ground states associated with strong quantum fluctuation effects. Later, a more practical aspect came to light when quantum spin fluctuations were suggested as possible mediators for unconventional pairing in some superconductors, most notably in the quasi-2D high-temperature cuprates [2].

The architecture of quasi-planar structures by linking CuO₄ squares which share common oxygen positions was first considered by Müller-Buschbaum [3] on an empirical basis (long before the high- T_c cuprate superconductors were discovered). Composing the basic CuO₄ units like bricks from a toy box leads to more and more complex networks with an intriguing variety of magnetic ground states. A few possible arrangements are sketched in Fig. 2. Isolated CuO₄ squares (Fig. 2a) can be present in connection with complex anions such as sulfate or phosphate groups like in the crystal structures of CuPbSO₄(OH)₂ and Sr₂Cu(PO₄)₂

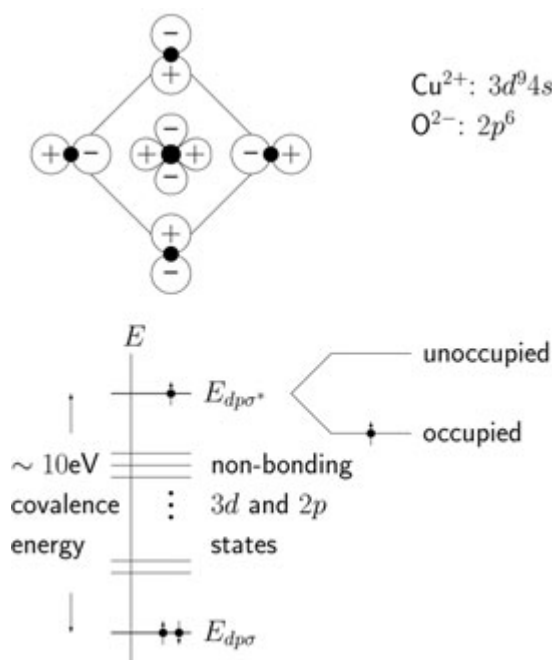


Fig. 1: Top) The covalent CuO₄ square, relevant for the cuprates. The copper ion resides in the center of the square, and the four oxygen ions occupy the corners. The antibonding molecular orbital is shown with sign changes of the wave function on all four Cu–O bonds, so that the wave function has nodes on the bonds. Bottom) molecular orbital scheme of the covalent CuO₄ square, the half-filled antibonding level is split due to strong on-site Coulomb correlations.

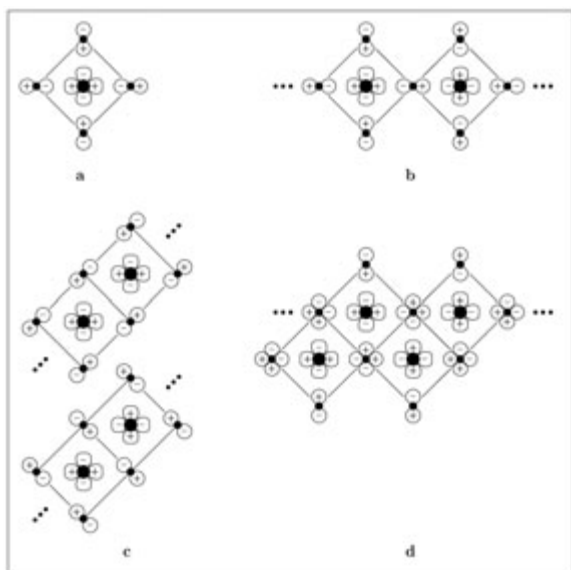


Fig. 2: Cuprate chains formed from the square (a) as the building block. A corner shared chain (b), an edge shared chain (c), and a double-chain (d) are shown. The phase factors of the orbitals correspond to the anti-bonding state.

[5], respectively. In other compounds CuO_4 squares may share common oxygen positions forming structural arrangements as sketched in Fig. 2b-d. Depending on the number of shared oxygen atoms, they can form corner shared chains (see Fig. 2b), edge shared chains (Fig. 2c) or double chains (Fig. 2d). By combination of the chains a rich variety of two-, three- or multi-leg ladders can be built [4]. In this way, a quasi-continuous transition is possible from 1D to 2D Cu(II)-compounds. Thus, a better understanding of the electronic and magnetic properties of quasi 1D chain compounds can be a key for deeper understanding of the high-temperature oxide-superconductors.

To extract the main ingredients for the electronic and magnetic properties of real compounds, density functional (DFT) calculations are a valuable tool. From the calculated electronic structure, the involved orbitals and the leading interactions can be estimated in terms of a tight-binding (TB) model. Subsequently, such TB model can be mapped to an extended Hubbard or Heisenberg model to improve the description of the above mentioned strong intra-atomic correlations at the Cu sites. From the approximate solution of such models, the magnetic ground state and its excitations can be estimated. In the following, this procedure is demonstrated exemplarily by the compounds $\text{Sr}_2\text{Cu}(\text{PO}_4)_2$ [5] and ACu_2O_2 ($A = \text{Na}, \text{Li}$) [6-10].

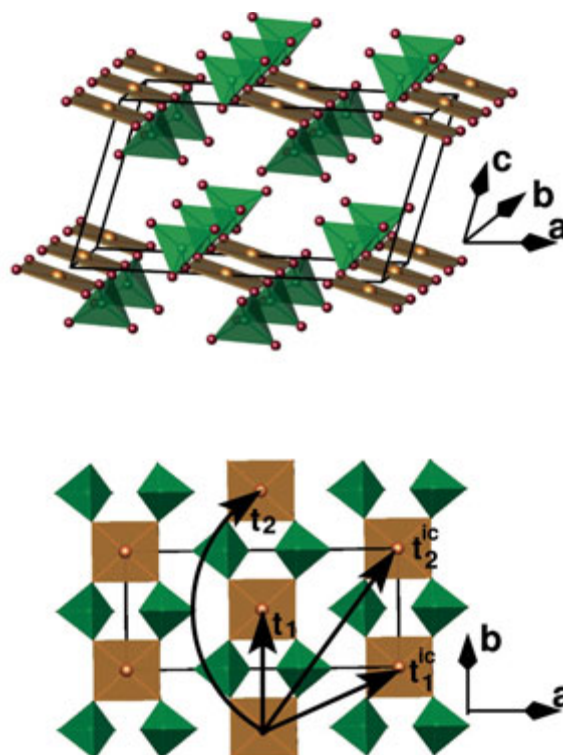


Fig. 3: Top) The crystal structure of $\text{Sr}_2[\text{Cu}(\text{PO}_4)_2]$ showing the isolated CuO_4 squares from which the Heisenberg spin chains are formed. Bottom) A top view of the spin chain plane with the various electronic hopping paths labelled. Hopping in the out-of-page direction is not shown.

$\text{Sr}_2\text{Cu}(\text{PO}_4)_2$ and the isotypic $\text{Ba}_2\text{Cu}(\text{PO}_4)_2$ exhibit a structural arrangement which is unique among known quasi-1D chains (see Fig. 3): planar CuO_4 squares are isolated from each other, and are linked by PO_4 tetrahedra to form infinite chains. Nearest neighbor squares are coplanar and run along [010] which represents the chain direction. CuO_4 -squares of adjacent chains (along [100]) occupy the positions “between” the squares of neighboring chains on both sides. Along [001] adjacent chains are separated by the full length of the unit cell parameter. Taking into account the structural details of $\text{Sr}_2\text{Cu}(\text{PO}_4)_2$ the compound would be best described as phosphato-cuprate (II) with the anionic partial structure given by $[\text{Cu}(\text{PO}_4)_2]^{4-}$.

Band structure calculations have been carried out within the local density approximation (LDA) using the full-potential local orbital code, FPLO [11]. The paramagnetic band structure of $\text{Sr}_2[\text{Cu}(\text{PO}_4)_2]$ (Fig. 4) shows a single half filled band, derived from the Cu $3d_{x^2-y^2}$ orbital, crossing the Fermi energy. Only the inclusion of strong electron corre-

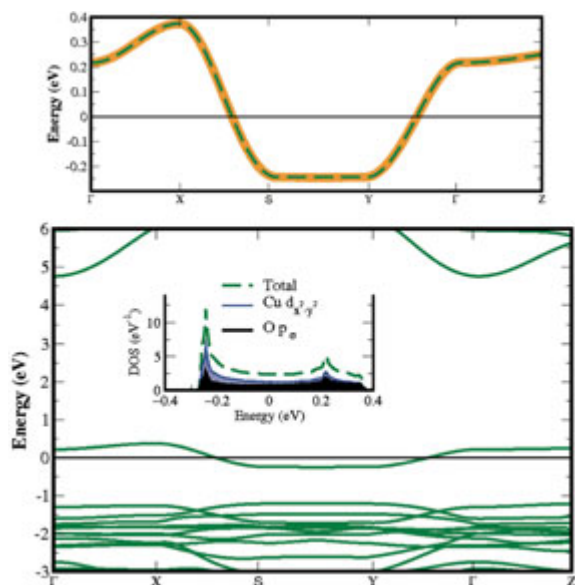


Fig. 4: The band structure of $\text{Sr}_2[\text{Cu}(\text{PO}_4)_2]$, showing the single metallic band well separated from all others. The X-S direction is along the magnetic chain, S-Y and Γ -Z directions are perpendicular to the chain. In the top panel, a blow-up of this band is shown with tight-binding eigenvalues superimposed to show the remarkable reproduction of the dispersion. The inset shows the total and orbitally resolved DOS for the single band.

lations leads to the insulating behavior which is experimentally observed. The 1D character of the system is qualitatively obvious from the nearly dispersionless bands in directions S-Y and Γ -Z which are perpendicular to the chain direction, and from the characteristic logarithmic divergences in the density of states (DOS) near the band edges (Fig. 4 inset). To quantitatively compare microscopic magnetic interactions, we fitted a tight-binding (TB) model to our band structure and calculated the individual exchange constants between various Cu spins using $J_{ij} = 4t_{ij}^2/U$ with a standard $U = 4.5$ eV. The hopping parameters included in the model are shown schematically in Fig. 3 (bottom). The resulting TB dispersion is indistinguishable from the full-potential calculation (Fig. 4 top), indicating that further interactions can be safely ignored. The ratio of the strongest in-plane coupling to the strongest inter-chain coupling is $J_1/J_1^{\text{ic}} \sim 70$ and the ratio of first to second neighbor in-chain coupling is $J_1/J_2 \sim 700$ for $\text{Sr}_2\text{Cu}(\text{PO}_4)_2$. Identical calculations based on the band structure of $\text{Ba}_2[\text{Cu}(\text{PO}_4)_2]$ (not shown) yield similar results with slightly more inter-chain coupling but less second neighbor in-chain coupling. Both systems can therefore be considered as strongly one-dimensional, with $\text{Ba}_2[\text{Cu}(\text{PO}_4)_2]$

slightly less so. These results are confirmed by additional LDA+U calculations.

The one-dimensional nature of magnetic interactions in $\text{Sr}_2[\text{Cu}(\text{PO}_4)_2]$ can be traced back to the isolated CuO_4 -squares. This construction virtually eliminates the second neighbor in-chain coupling that prevents compounds such as Li_2CuO_2 from being described via a simple nearest neighbor Heisenberg model [12,13]. Cuprates such as Sr_2CuO_3 containing corner-sharing CuO_4 squares have far smaller second neighbor interactions, of the order $J_1/J_2 \sim 15$, and yet, these must be taken into account to get good agreement between model calculations and experiment [14]. Conceptualized in this way, one can make a correspondence between exchange constants in edge-sharing CuO_4 -systems (es) and those with isolated CuO_4 -squares (i): $J_2^{\text{es}} \rightarrow J_1^{\text{i}}$, and $J_4^{\text{es}} \rightarrow J_2^{\text{i}}$. Since J_4^{es} is known to be vanishingly small, it is clear that the second neighbor interactions between isolated squares can be expected to be negligible.

Of course, experiment will be the final arbiter of the degree of one-dimensionality in $\text{Sr}_2[\text{Cu}(\text{PO}_4)_2]$. New experimental results confirm an extraordinary one-dimensionality with no long range order setting in even into the mK temperature range. Low temperature thermodynamic measurements down to 30 mK show long range order only below $T_N = 0.085$ K. This temperature is about 2000 times smaller than the leading interaction J_1 along the chain, showing that quantum fluctuations dominate the low temperature magnetic properties of this system.

We have shown that the isolated CuO_4 squares in $\text{Sr}_2[\text{Cu}(\text{PO}_4)_2]$ allow for an excellent description of its magnetic and thermodynamic properties using a 1D nearest neighbor only Heisenberg spin $1/2$ model. We calculated the exchange constant and extracted it from experimental data and found extremely good agreement between the two. $\text{Sr}_2[\text{Cu}(\text{PO}_4)_2]$ is the best realization for the 1D nearest neighbor Heisenberg model so far. We anticipate that $\text{Sr}_2[\text{Cu}(\text{PO}_4)_2]$ will be useful as a real physical system that can be compared to theoretical models with confidence that deviations from prediction are due to actual effects beyond the Heisenberg Hamiltonian rather than to non-1D or distant neighbor interactions.

Another example for the realization of an unusual magnetic ground state are the isostructural compounds LiCu_2O_2 and NaCu_2O_2 which exhibit a hel-

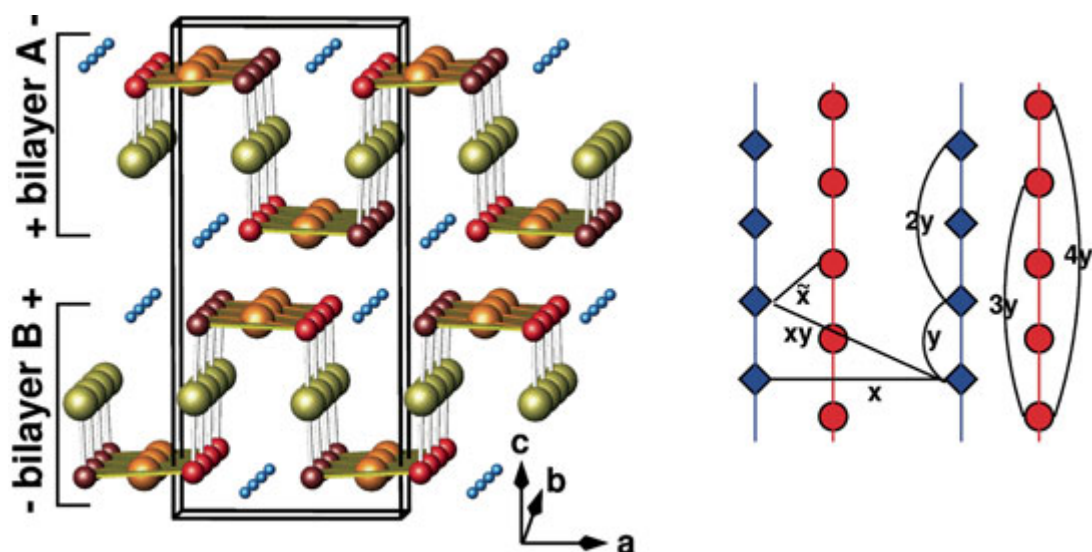


Fig. 5: Left) Crystal structure of ACu_2O_2 ($A = Na, Li$) with two bilayers of CuO_2 chains running along b (Cu^{II} orange, Cu^{I} yellow, inner (outer) O red (brown), Na blue). Right) Schematic chain structure with the main exchange paths indicated. Filled diamonds and circles denote CuO_2 squares in A and B bilayers, respectively

ical magnetic order at low temperatures [6-10]. The crystal structure of $LiCu_2O_2$ and $NaCu_2O_2$ is shown in Fig. 5 and consists of bilayers of edge-sharing $Cu^{II}O_{4/2}$ -chains that run along the crystallographic b axis. The $Cu^{II}O_{4/2}$ -chains are linked by non-magnetic $Cu^IO_{2/2}$ dumb-bells thus forming the bilayer. Similarly to $Sr_2[Cu(PO_4)_2]$, we mapped the LDA band structure (not shown) of this system to a TB model, shown in the right panel of Fig. 5. In contrast to $Sr_2[Cu(PO_4)_2]$, we find dominating second neighbor interactions and a considerable inter-chain coupling. Including the ferromagnetic component of the nearest neighbor exchange J_1 arising from the almost 90° $Cu^{II}-O-Cu^{II}$ bond angle along the chains, we end up with competing magnetic interactions along the $Cu^{II}O_{4/2}$ chain: ferromagnetic $J_1 \sim -50$ K and antiferromagnetic $J_2 \sim +100$ K. This competition leads to strong magnetic frustration and, as predicted from model calculations, to a helimagnetic order along the chains in agreement with the experimental observations.

Recently, we investigated the magnetic properties of $Cu_2[PO_6(CH_2)]$ [15]. From the structural point of view, this compound is situated in “between” the systems discussed above. It consists of isolated dimers ($O_2CuO_2CuO_2$), formed by two CuO_4 units sharing a common edge. The long axes of the dimers are arranged in direction of the crystallographic b axis (see Fig. 6). The dimers are significantly distorted and connected via $O_3P(CH_2)PO_3$ -groups. Preliminary experimental and theoretical

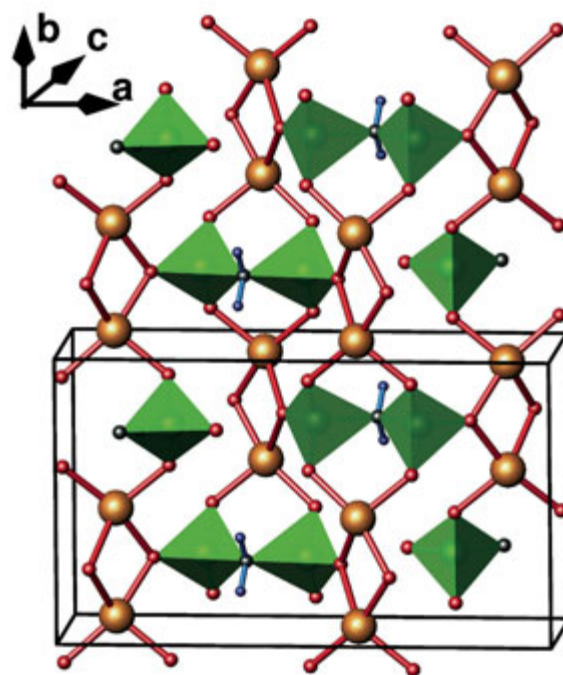


Fig. 6: Crystal structure of $Cu[PO_6(CH_2)]$. The CuO_4 units form distorted dimers which are linked via $O_3PCH_2PO_3$ groups (green).

results indicate that this compound exhibits a spin gap at low temperatures. To clarify the nature of the magnetic coupling and the exact mechanism for the spin gap formation, further investigations on single crystals will be required.

We have shown that the magnetic properties of low dimensional Cu^{II} -compounds strongly depend

on details of their crystal structures. Using complex oxo-anions of non-metals (e.g. B, C, P, S...) as space- and direction-controlling agents for Cu^{II}-coordination squares (and their interconnections) a large variety of compounds with intriguing magnetic properties could be constructed and prepared. Thus, we expect that the combination of theoretical electronic structure calculations, thermodynamic and spectroscopic investigations together with well-directed crystal chemical aspects will be a powerful tool for future exploration of quantum phase diagrams of low dimensional materials.

References

- [1] *L. Onsager*, Phys. Rev. **65** (1944) 117.
 [2] *J. P. Carbotte, E. Schachinger, and N.D. Basov*, Nature **401** (1999) 354.
 [3] *H. Müller-Buschbaum*, Angew. Chem. **89** (1977) 704.
 [4] *E. Dagotto and T. M. Rice*, Science **271** (1996) 618.
 [5] *M.D. Johannes, J. Richter, S.-L. Drechsler, A. A. Belik, E. Takayama-Muromachi, S. Uji, T. Terashima, and H. Rosner*, to be published.
 [6] *T. Masuda, A. Zheludev, A. Bush, M. Markina, and A. Vasiliev*, Phys. Rev. Lett. **92** (2004) 77201.
 [7] *A. A. Gippius, E. N. Morozova, A. S. Moskvina, A. V. Zalessky, A. A. Bush, M. Baenitz, H. Rosner, and S.-L. Drechsler*, Phys. Rev. B **70** (2004) 020406.
 [8] *S.-L. Drechsler, J. Málek, J. Richter, A. S. Moskvina, A. A. Gippius, and H. Rosner*, Phys. Rev. Lett. **94** (2005) 039705.
 [9] *L. Capogna, M. Mayr, P. Horsch, M. Raichle, R.K. Kremer, M. Sonin, and B. Keimer*, Phys. Rev. B **71**, (2005) 140402.
 [10] *S.-L. Drechsler, J. Richter, A.A. Gippius, A. Vasiliev, A. A. Bush, A. S. Moskvina, J. Málek, Y. Prots, W. Schnelle, and H. Rosner*, Europhys. Lett., in press.
 [11] *K. Koepf and H. Eschrig*, Phys. Rev. B **59** (1999) 1743.
 [12] *R. Weht and W. E. Pickett*, Phys. Rev., Lett. **81** (1998) 2502.
 [13] *R. Neudert, H. Rosner, S.-L. Drechsler, M. Kiewein, M. Sing, M. Knupfer, M. S. Golden, J. Fink, N. Nücker, S. Schuppler, N. Motoyama, H. Eisaki, S. Uchida, Z. Hu, M. Domke, and G. Kaindl*, Phys. Rev. B **60** (1999) 13413.
 [14] *H. Rosner, H. Eschrig, R. Hayn, S.-L. Drechsler, and J. Malek*, Phys. Rev. B **56** (1997) 3412.
 [15] *H. Rosner, M. Schmitt, W. Schnelle, A. Gippius, W. Liu, Y. Huang, and R. Knipf*, in preparation.

¹ Naval Research Laboratory, Washington, USA

² Leibniz-Institut für Festkörper und Werkstofforschung, Dresden, Germany